Controlling Plume Divergence in a Cusped-Field Thruster

IEPC-2011-178

Presented at the 32^{nd} International Electric Propulsion Conference,
Wiesbaden, Germany
September 11–15, 2011

Taylor S. Matlock* Fuzhou Hu† and Manuel Martinez-Sanchez‡
Massachusetts Institute of Technology, Cambridge, Massachusetts, 02139, USA

The Diverging Cusped-Field Thruster (DCFT) uses three rings of alternating polarity permanent magnets to create a set of axial and para-radial cusps which serve to impede electron motion to a centrally mounted rear anode and to protect the electrically insulating walls of the discharge chamber. Measurements have shown that the majority of ion acceleration in this thruster occurs near the exit separatrix, the null magnetic potential line separating the magnetic region external to the discharge chamber from an upstream internal magnetic cell. It is hypothesized that the placement of the cathode in a high magnetic vector potential combined with the low neutral densities downstream of the exit lead to a large local electron impedance between the cathode and exit separatrix. An electron is already at a low magnetic potential as it passes through the separatrix into the internal magnetic cell and will likely encounter less resistance as it travels towards the anode. The differences in impedance provide a simplified description of the thruster, analogous to a voltage divider, in which the majority of the potential drop will occur downstream of the exit.

An externally mounted electromagnet was designed and built to directly modify the shape of the exit separatrix and the external field in general in order to asses how changes in the exit topology can be used to manipulate the divergence of the plasma plume. A Faraday probe and Retarding Potential Analyzer are used to measure the ion flux and ion energy distribution dependencies on angle from the thrust axis for a range of thruster operating conditions and magnetic field settings. The angle of the peak ion flux is found to decrease by more than 5° when a large additional field is imposed near the exit by the electromagnet, effectively bending the separatrix back towards the upstream direction. The additive fields imposed by the electromagnet were also shown to decrease the anode current in a manner perhaps partly analogous to the anode current optimization in Hall thrusters.

*Graduate Student, Department of Aeronautics and Astronautics, tmatlock@mit.edu.
†Undergraduate, Department of Aeronautics and Astronautics.
‡Professor. Department of Aeronautics and Astronautics, mmart@mit.edu.

Nomenclature

e = elementary charge
I_{an} = anode current
I_b = total ion current in plume
I_{mag} = current supplied to external electromagnet
I_p = collected probe current
$\dot{m}$ = propellant mass flow rate
m_i = ion mass
η_b = beam efficiency I_b/I_{an}
η_u = propellant utilization efficiency $m_i I_b/(e\dot{m})$
θ = angle from thruster axis of symmetry

I. Introduction

The past decade has shown the emergence of several gridless plasma thrusters utilizing some form cusped magnetic field to inhibit plasma losses to discharge chamber surfaces, in the hopes of providing at least comparable performance to similar class Hall thrusters while increasing the total impulse deliverable before insulator erosion effectively ends the life of the device. Among the various cusped-field devices, the Thales HEMP-thruster,[1] Princeton's permanent magnet CHT[2] and the Diverging Cusped Field Thruster (DCFT) being investigated in different forms at MIT[3] and Stanford,[4] there has been the collective observance of a nearly hollow, conical plume structure, where the ion beam is largely focused into a shell which is peaked on the order of 30° to 50° from the thruster axis-of-symmetry (though this is no longer the case in more recent versions of the HEMP-T[5]). The ions within this shell have been measured by many to be accelerated by nearly the entire applied potential, while in several cases, retarding potential analyzers (RPA's) revealed the ion fluxes nearer to the centerline to be of a generally lower energy composition.[2,6,7]

A conventional Hall thruster plume, in comparison, is peaked within a few degrees of the thruster axis and decays roughly exponentially at higher angles. In a simplified sense, the magnetic flux lines in a Hall thruster can be considered to very roughly coincide with lines of equipotential, with some defocussing due to electron pressure and wall interaction, as presented in a review of Hall thruster physics by Morozov and Savelev.[8] Under these premises it is clear how adding some concavity (where concavity refers to a radius of curvature pointing towards the anode) to the flux lines near the ionization/acceleration region of the channel can help focus the ion beam towards the centerline, and such an effect has been observed in experiment.[9]

Though there are best-practices for creating a focused plume in a Hall thruster, the issue has not been universally clarified in the cusped-field thruster literature. The magnetic field topology of the DCFT, shown in Fig. 1, differs quite distinctly from that in a conventional Hall thruster and initially it was unclear where the main region of ionization or acceleration would occur. Emissive probe measurements in the near-field of a cylindrical variant of the DCFT performed by Young *et al*[4] showed a drop in the plasma potential downstream of the exit accounting for a significant portion of the applied voltage. Similar measurements were then made on the DCFT at MIT which also suggested the majority of the potential drop sits near the exit and a hypothesis for the role of the magnetic topology in anchoring acceleration to this region was discussed.[10]

The crux of the argument is that electrons are expected to have a difficult time crossing the strong magnetic field at the exit to gain access to the internal discharge chamber, but once inside they are already on a field line which connects directly to the next upstream separatrix. The high local impedance to axial electron motion then allows an electric field to form, unshielded, across the field lines leading up to the exit separatrix. A slightly different explanation was forwarded in an earlier paper by Kornfeld *et al* to account for the observed peak in electric field at the exit of the HEMP Thruster,[1] where the low neutral density and peak mirror ratio at the exit ring cusp were given as the main impediments to axial electron flow. Whatever the mechanism for cross field electron transport, it seemed clear to us that the commencement of the large potential drop should lie close to the ultimate separatrix, upstream of which electrons are relatively free to flow axially until perhaps being mirrored further on by the point cusp. Indeed this has been borne out by recent laser induced fluorescence (LIF) measurements of the ion velocity in the near-exit region of the DCFT by MacDonald *et al*,[11] which show a rather pronounced localization of ion acceleration around the final separating field line. It then became the focus of the experiment described herein to attempt to lower the divergence of the ion plume in the DCFT by making the downstream separatrix less convex, and thus hopefully forcing a more axially pointing peak electric field.

The following section describes the experimental setup in which an electromagnet is placed flush with the thruster exit and used to modify the shape of the final separatrix. A Faraday probe is used to measure any changes in the spatial distribution of ion current density in the far-plume and a Retarding Potential Analyzer (RPA) is implemented to check whether the magnetic field alterations result in drastic differences in the energy composition of the ions in the plume. The results discussed below show clearly that the decreased convexity of flux lines near the exit is accompanied by a shift in a large portion of the ion flux to smaller angles. RPA measurements are somewhat hampered by some experimental oddities discussed in the following section, but the results do not suggest there is any noticeable change in the ion energy distribution when the near-field magnetic topology is altered.

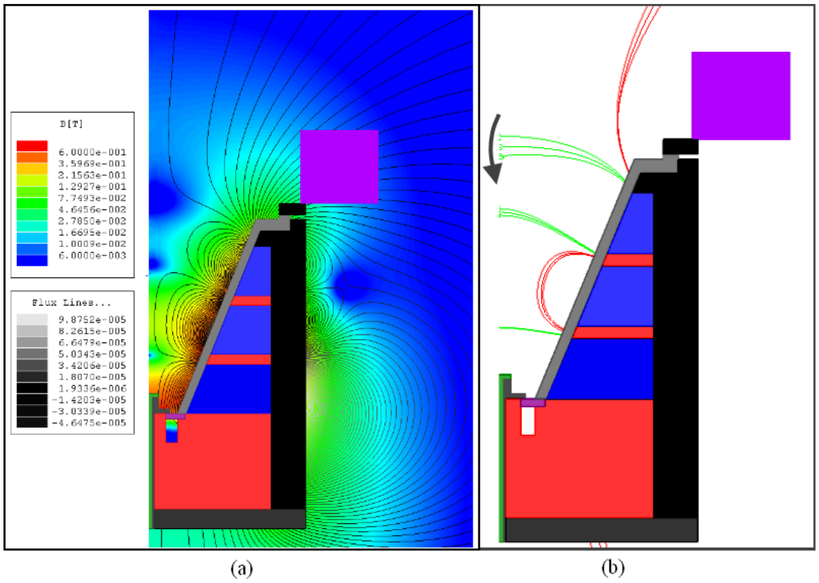

Figure 1. Ansoft Maxwell SV simulations of the DCFT outfitted with electromagnet (shown in purple). Field strength and flux lines are shown in (a) with 0 A to magnet and (b) with just flux lines highlighting the separatrices at various magnet currents in green. An arrow shows the direction the exit separatrix moves as the magnet current is increased from 0 A to 10 A then 20 A.

II. Experimental Apparatus

The electromagnet used in this experiment has an 8 cm inner diameter and is roughly 2 cm long including support structure. The enamel-coated copper coil consists of roughly 30 turns and is powered by an Agilent N5761A to not much in excess of 25 A in order to avoid overheating. In the intended polarity the magnet is able to provide a sufficient counter-field to bend the field lines near the thruster exit back towards the anode as shown in Fig. 1(b) where commercial software is used to predict the flux line topology for different electromagnet input currents, I_{mag}. The figure also shows that electromagnet has little effect on the shape of the separatrix near the discharge chamber walls where the field is much higher than that the coil can produce. Measurements of the magnetic field in the thruster at different coil currents have been performed with an AlphaLabs Inc. DC Gaussmeter and are shown in the Appendix.

Of course, the electromagnet not only changes the shape of the separatrices, it significantly alters the strength of the magnetic field near the exit. The measured effects are shown in Fig. 6 where it is clear that the electromagnet strengthens the field downstream of the exit, while weakening the point cusp just upstream of the exit. A strong exit magnetic field has been hypothesized as the culprit for large beam divergence in a permanent magnet CHT,[2] so the effects of the change in topology and change in field strength here may be mixed. The inner surface of the electromagnet is covered with Kapton tape to provide thermal and electrical insulation to the magnet support structure, and perhaps most importantly to prevent sputtering and redeposition of the conductive aluminum.

Experiments were performed inside the MIT Space Propulsion Laboratory ASTROVAC vacuum chamber. The chamber is roughly 1.5 by 1.6 m with a pumping speed of about 7500 L/s on Argon obtained using two CTI-Cryogenics cryopumps (CT10 and OB400). Pressure in the chamber is monitored using an inverted magnetron gauge, and is seen to vary between pressures of around 20 to 50 μTorr at the flow rates of xenon used in the experiment described here. A Busek Inc. cathode is used as an electron source to initiate the discharge and neutralize the resulting ion beam.

The DCFT operates in either a high current mode with strong anode current oscillations around 1-5kHz, or a low current quiescent mode. The high current (HC) mode is a bifurcation marked by a steep jump in anode current as (generally) either the mass flow is increased or the anode potential is turned down, resulting in a visually diffuse plume. The low current (LC) mode has a visually distinct plume with the apparent coalescence of the ion beam to an angle of around 30-40° from the thruster centerline.

The thruster body is left electrically floating, while the anode and cathode keeper potentials are applied with respect to the common chamber and facility ground. The anode voltage is set by an Agilent N5772A

Programmable Power Supply, while the keeper current is set by a Sorensen DCS 600-1.7. Flow control and measurement to the anode and cathode is provided by two Omega FMA-A2400 series mass flow controllers, allowing 0-10 mL/min flows calibrated for Xenon. The cathode is generally run at a 0.5 A keeper current with 0.1 mg/s of xenon, however keeper currents of up to 1.3 A and cathode flows of up to 0.2 mg/s are found in this experiment to be necessary for stable operation in LC mode.

Probes are positioned within the chamber by a stack of two linear translation stages forming an X-Z system and a rotational stage driven by a set of stepper motors. The X stage positions the probes to a certain radial distance from the thruster centerline and has a total travel length of 30in. The 40in-long Z stage controls the axial position of the probe with the face of the aluminum cap bolted to the thruster exit taken as Z=0. The step resolution of both stages is 5μm. The stages are controlled through LabView using a Velmex Inc. VXM motor controller. The experiments described here use the three stages to mimic a swinging boom with its pivot at a point on the intersection of the exit plane and the vertical plane containing the thruster axis and cathode exit. Spatial scans of the plume are performed a distance of 38 cm from the pivot at angles of up to 70° from the centerline.

Heritage Faraday and RPA probes are used, the design of which is described elsewhere.[12] Both collect ion current on a circular plate of 4.5 mm diameter. The Faraday probe guard ring and collector are biased 27 V below ground using a series of 9 V batteries and the current to the collector is measured on the high side of the applied voltage through a 2 kΩ resistor using a Fluke 77 IV handheld meter.

The RPA consists of a series of molybdenum grids of 72% open area, with 0.14 mm wide hexagonal openings. The first grid (counting up going downstream) is left floating along with the thruster body, the second is normally set to -27 V in order to repel electrons and the third is connected to a Bertan 230S, 5 kV bi-polar power supply used to selectively deflect ions based on their directed energy. The distance between the electron repelling and ion retarding grids is only 0.5 mm in an attempt to avoid space charge effects on the extracted current. The RPA current is measured using a Keithley 2410 SourceMeter which averages 10 samples per retarding voltage set point. Data collection and probe movement are coordinated using LabView.

The RPA used in this experiment exhibited some rather unexpected characteristics. When the electron repelling grid was biased below ground the ion repelling grid power supply (Bertan 230S) would not go below some high potential (around 100 V), however when the electron repelling grid was allowed to float, the ion repeller would sit near 15 V until programmed to higher voltages. As a result, data describing the low energy component of the ion distribution were not available with the electron repeller in its normal configuration. The effects of this odd operation on the data are unkown and an external form of verification is needed.

A two-axis stage is also used to position the cathode during experiments. The nominal cathode position is about 7 cm radially from the thruster axis, and 3 cm downstream of the exit. The electromagnet occludes the flux line which connects this nominal cathode location to the discharge chamber and so a different position is needed. The stages allow in situ adjustment of the cathode position which demonstrably affects the stability of the different regimes of thruster operation. In fact, much of the RPA data in LC mode are taken with the cathode very nearly on the edge of the main jet emanating at roughly 30°, as moving the cathode much closer to or much farther from the axis was found to result in a highly repeatable change into HC mode.

III. Results and Discussion

Powering the electromagnet leads to a noticeable change in the anode current and at some conditions, a repeatable switch in operational regime from LC to HC mode. In general, an increase in magnet current leads to a decrease in the anode current until a minimum is reached (usually between 5 A and 20 A) above which the added magnet current leads to an increase in anode current and in anode current oscillations. The oscillations generally start as a flickering between a quiet LC mode and the HC mode containing periodic peaks in anode current, but at magnet currents above 20 to 25 A a stable HC mode is usually obtained. Example curves of anode current as a function of magnet current are given in Fig. 2 for different anode voltages at an anode flow rate of 0.49 mg/s and a 1.0 A keeper current. As the figure demonstrates, the minimum anode current is a significantly smaller percentage of the normal current and is achieved at a much larger magnet current when the anode voltage is low at these conditions. This trend is not universal, however, with recent testing showing a continual decrease in anode current up to a 20 A magnet current for a mass flow rate of 0.68 mg/s at 450 V.

The thruster is run at a variety of flow rates, anode voltages and cathode locations all exhibiting the

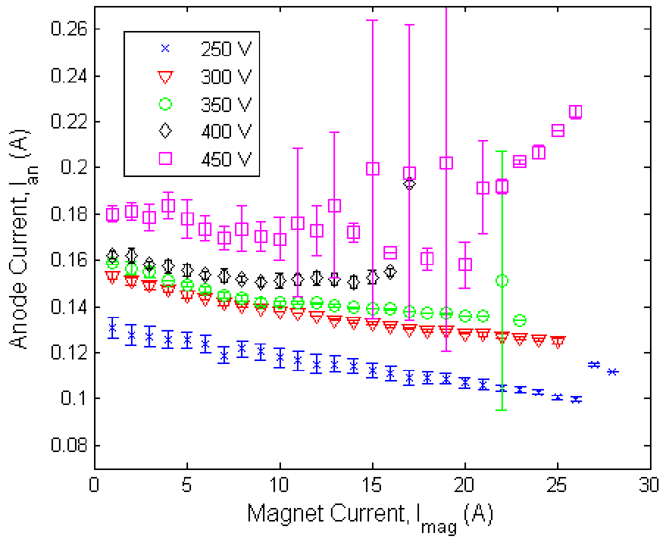

Figure 2. Average anode current at a given electromagnet current at a 0.49 mg/s anode mass flow rate and 1.0 A keeper current for various anode voltages. Error bars denote one standard deviation.

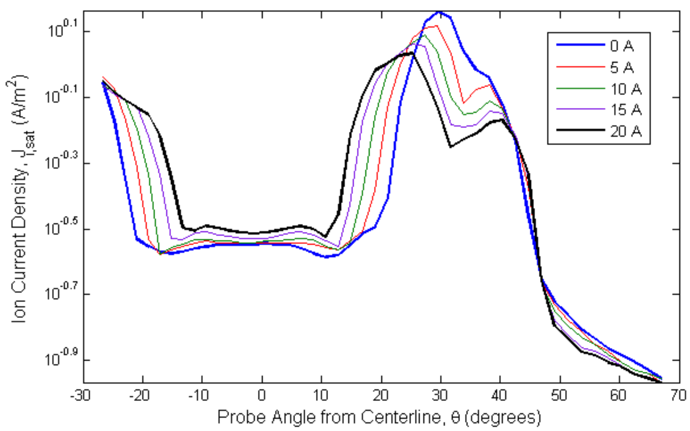

Figure 3. Faraday probe measured ion saturation current at 300 V and 0.49 mg/s of xenon for various magnet currents (0-20 A) at 38 cm.

same trend in Faraday probe measured ion current peak with applied magnet current. The resulting plume profile is shown in Fig. 3 with the thruster operated at 300 V, 0.49 mg/s of xenon to the anode, 98μg/s to the cathode, a keeper current of 1.275 A, and magnet currents ranging from 0 to 20 A, resulting in anode currents from 268 mA to 232 mA. The figure shows a smooth progression of the location of peak ion current density in the plume from an angle of 30° down to an angle of about 25° as the magnet current is stepped in 5 A increments from 0 to 20 A. Meanwhile, a secondary peak remains at around 38° from the thruster axis, which appears to slightly shift outwards to about 40° at the maximum magnet current. Other apparent trends are the slight increase in ion current at angles less than the peak current location and the slight decrease in ion current to the probe at angles greater than 47° as the magnet current is raised.

The apparent splitting of the beam into nested shells emanating at about 25° and 40° is also observable in visual examination of the plume and may be due in part to the fact that the electromagnet is only able to affect the field line convexity away from the wall where the field is relatively weak. The reason why the plume is marked by two discrete beamlets and not a more continuous structure is unclear. One might be tempted to conclude that the more divergent beamlet is actually originating from the next upstream separatrix, which is gradually made more convex by the the electromagnet. This idea is not well supported by experimental evidence, however, with LIF measurements of the axial velocity near the second separatrix

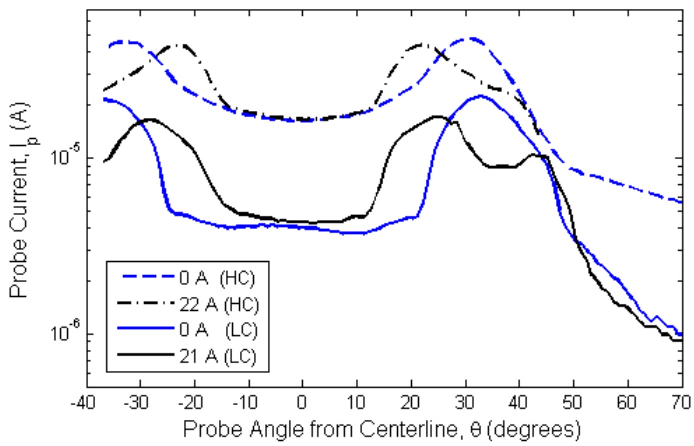

Figure 4. Faraday probe measured ion saturation current at 300 V and 0.59 mg/s of xenon in LC mode and 0.68 mg/s in HC mode for various magnet currents (0 to 22 A) at 38 cm.

showing that ions move very slowly in this region,[11] and all RPA data from around 40° suggesting a nearly identical ion energy composition as is found in the more prominent jet at 30°. A splitting of the beam is seen in both LC and HC modes as shown in Fig. 4, where the HC mode is obtained at 0.68 mg/s and the LC mode occurs at 0.59 mg/s, both at anode voltages of 300 V.

Beam current can be estimated from the Faraday probe measurements using Eq. 1, where R is the probe arm length, θ is the angle between probe face normal and the thruster axis, J_i is the ion current density (approximated as the probe current divided by the physical area of the collector) and which assumes axial symmetry. The results of the integration show the beam current decreasing nearly linearly with applied magnet current, but the slope of this decrease is less than that of the roughly linear decrease in anode current which accompanies the effect. The result is an increased beam efficiency ($\eta_b = I_b/I_{an}$) at high magnet currents, however the drop in propellant utilization efficiency ($\eta_u = m_i I_b/(e\dot{m})$) is measured to be a larger effect, and the product of the two efficiencies actually decreases with exit magnetic field strength. The efficiency product drops linearly from 41% at 0 A to 37% at 20 A on the electromagnet for the LC case at 300 V and 0.49 mg/s to the anode shown in Fig. 3. This is not the full story, however, as the decreased beam divergence caused by the electromagnet leads to an efficiency gain from the normal $cos^2\theta$ term. The $cos^2\theta$ efficiency, estimated by taking the ion current averaged $cos\theta$, rises from 0.63 to 0.65 when the electromagnet current is increased from 0 A to 20 A. The product of all three efficiencies gives then a 2% drop in efficiency at the high magnet current, which is below the accumulated uncertainty in theses measurements. As a result, no firm conclusions are drawn as to the cumulative effect of the magnetic field change on efficiency.

$$I_b = 2\pi R^2 \int_0^{\pi/2} J_i(\theta) sin\theta d\theta \tag{1}$$

The measured increase in beam efficiency with exit magnetic field strength may be explainable from the corresponding impediment to electron cross-field transport limiting the backstreaming electron current, but the mechanism for the observed drop in propellant utilization is a bit more ambiguous since one might suspect that an increased field strength might increase the electron confinement time near the exit, allowing for more ionizing collisions. Alternatively, one may take the view where ionization still occurs near the separatrix, but it is mainly due to electrons trapped between the upstream point cusp and the the ring cusp at the chamber wall, since electrons downstream of the exit are less likely to bounce back towards the thruster once initially reflected towards the plume. In this view, the weakening of the point cusp which confines electrons to this region by the electromagnet could be the culprit for reduced ionization. A somewhat similar hypothesis is espoused in the HEMP thruster literature[1] in which the main ionization is thought to be carried out by electrons trapped by the most downstream internal point cusp, leading designers to lengthen this section of largely axial magnetic field in the hopes of increasing propellant utilization.

Of course, this is all quite speculative. The apparent decrease in beam current with magnet current may instead be due to a number of experimental factors, such as the limited angular range of the positioning system, the uncharacterized effect of charge exchange collisions with background chamber neutrals, or even

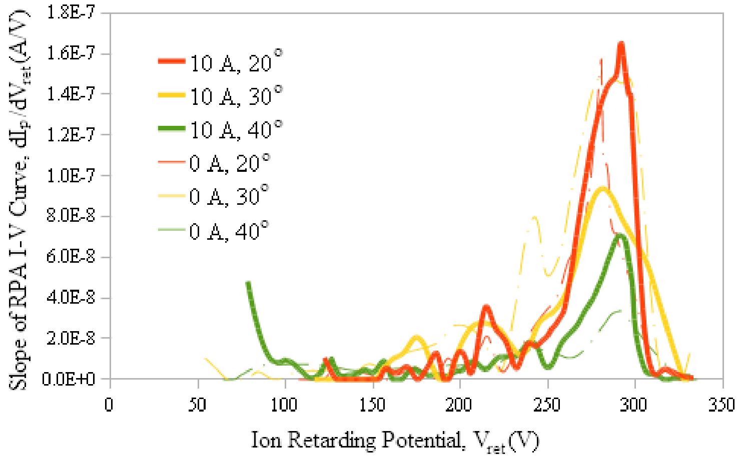

Figure 5. Derivative of RPA probe measured current with ion retarding potential versus ion retarding potential at various angles and magnet current settings. The thruster is operated in LC mode at 300 V a flow of 0.59 mg/s to the anode, 0.098 mg/s to the cathode and a keeper current of 1.25 A.

a defocussing of the outer edge of the ion beam by the magnetic field leading to recombination on the electromagnet itself.

According to the ordinary one-dimensional probe theory, the first derivative of the RPA collector current with the ion retarding voltage is proportional to the ion energy distribution function.[13] Cubic spline smoothed first derivatives of the RPA I-V curves are shown in Fig. 5 with the thruster at 300 V and a 0.59 mg/s anode flow for a discharge current of 320 mA with no magnet current and 312 mA with 10 A to the coil. The results suggest that at angles containing most of the ion flux (20° to 40°) the majority of ions have an energy per charge that is close to the applied potential, regardless of the application of magnet current. This needs to be verified more fully, but suggests that the lower divergence beamlet does not consist of ions born downstream of the main ionization/acceleration region.

IV. Conclusion

A preponderance of evidence suggests the main acceleration in cusped-field thrusters occurs near the exit regardless of operational mode and so our attempts to improve the axial collimation of the exiting ion beam have focused on reshaping the electric field by altering the magnetic field topology. The exit separatrix has been a natural focal point for our topology modifications as the surrounding flux lines bunch up nearby. Also, since cross field electron transport is no longer necessary for axial electron motion upstream of this boundary it may denote the upstream edge of the main potential drop.

By placing an electromagnet at the exit of the thruster we have been able to decrease the convexity of the exit separatrix near the thruster axis and have demonstrated the effectiveness of this approach in decreasing the divergence of the plume by measuring ion flux properties in the far-field using RPA and Faraday probes under various configurations of vacuum magnetic field. An unexpected effect of the external magnet is observed where high magnet currents lead to a stratification of the plume into a pair of nested shells. The inner shell can be vectored inward from upwards of 30° down to around 25° while the outer shell remains nearly constant at a 40° from the thruster centerline.

Unfortunately, the presence of the electromagnet itself has an unquantified effect on the crucial near-exit plasma. The neutral propellant gas no longer expands to vacuum past the exit plane, but instead is contained in an 8 cm diameter, 2 cm long extension. The impingement of ions on the electromagnet leads to recombination which further enhances the neutral density in this region. The inner surface of the magnet also provides an insulated boundary to the exiting plasma which will certainly change the plasma dynamics, though the extent may be limited. Plasma potential measurements inside the electromagnet, if feasible, could provide some insight into how the plasma is redistributing itself in the presence of the magnet and the added magnetic field. Of course, the effect of electromagnet impingement can be removed entirely if a new thruster prototype is built with the desired field topology created using permanent magnets instead.

Appendix: Magnetic Field Measurements

The magnetic field was measured using an AlphaLabs Inc. DC Gaussmeter and positioned using the 3-axis system used for probe positioning with the thruster in its experimental condition in ASTROVAC. The probe sensor area for the Gaussmeter is 4 mm by 1.5 mm with the uncertainty in probe angle being the largest contributor to errors in the measurements. Measured field strengths and flux line topology are shown in Fig. 6 for 0 A, 10 A and 20 A supplied to the electromagnet. The expected effect of increased coil current reducing the convexity of the separatrix near the thruster axis is clearly verified by the measurements. Flux lines are interpolated from the measurements using Tecplot 360 software.

Acknowledgments

The work described here was funded under a grant from the Air Force Office of Scientific Research. The authors would like to thank Stephen Gildea and Prof. Paulo Lozano for their thoughtful discussion.

References

[1]Kornfeld, G., Koch, N., Harmann, H. "Physics and Evolution of HEMP-Thrusters", *30th International Electric Propulsion Conference*, 2007.

[2]Raitses, Y., Merino, E., Fisch, N.J. "Cylindrical Hall thrusters with permanent magnets", *Journ Appl Phys* Vol. 108 (093307), 2010.

[3]Courtney, D., Martinez-Sanchez, M. "Diverging Cusped-Field Hall Thruster (DCHT)", *30th International Electric Propulsion Conference*, 2007.

[4]Young, C., Smith, A., Cappelli, M. "Preliminary Characterization of a Diverging Cusped Field (DCF) Thruster", 31st International Electric Propulsion Conference, 2009.

[5]Koch, N., Kornfeld, G., Harmann, H. "Status of the THALES High Efficiency Multi Stage Plasma Thruster Development for HEMP-T 3050 and HEMP-T 30250", *30th International Electric Propulsion Conference*, 2007.

[6]Kornfeld, G., Koch, N., Coustou, G. "First test results of the HEMP thruster concept", *28th International Electric Propulsion Conference*, 2003.

[7]Gildea, S., Martinez-Sanchez, M., Nakles, M., Hargus, W. "Experimentally Characterizing the Plume of a Divergent Cusped-Field Thruster", *31st International Electric Propulsion Conference*, 2009.

[8]Morozov, A.I., Savelyev, V.V. "Fundamentals of Stationary Plasma Thruster Theory" *Reviews of Plasma Phys* Vol. 21, 2000.

[9]Gavryshin, V.M., Kim, V., Kozlov, V.I., Maslennikov. "Physical and Technical Bases of the Modern SPT Development" *24th International Electric Propulsion Conference*, 1995.

[10]Matlock, T., Gildea, S., Hu, F., Becker, N., Lozano, P., Martinez-Sanchez, M. "Magnetic Field Effects on the Plume of a Diverging Cusped-Field Thruster", *46th AIAA/ASME/SAE/ASEE Joint Propulsion Conference*, 2010.

[11]MacDonald, N.A., Cappelli, M.A., Gildea, S.R., Martinez-Sanchez, M., Hargus Jr., W.A. "Laser-induced flourescence velocity measurements of a diverging cusped-field thruster", *J Phys D: Appl Phys* Vol. 44 (295203), 2011.

[12]Azziz, Y. "Experimental and Theoretical Characterization of a Hall Thruster Plume" Doctoral Dissertation, Department of Aeronautics and Astronautics, Massachusetts Institute of Technology, Cambridge, MA, 2007.

[13]Hutchinson, I.H *Principles of Plasma Diagnostics*, Cambridge University Press, Cambridge, UK, 2002, pp.97-98.

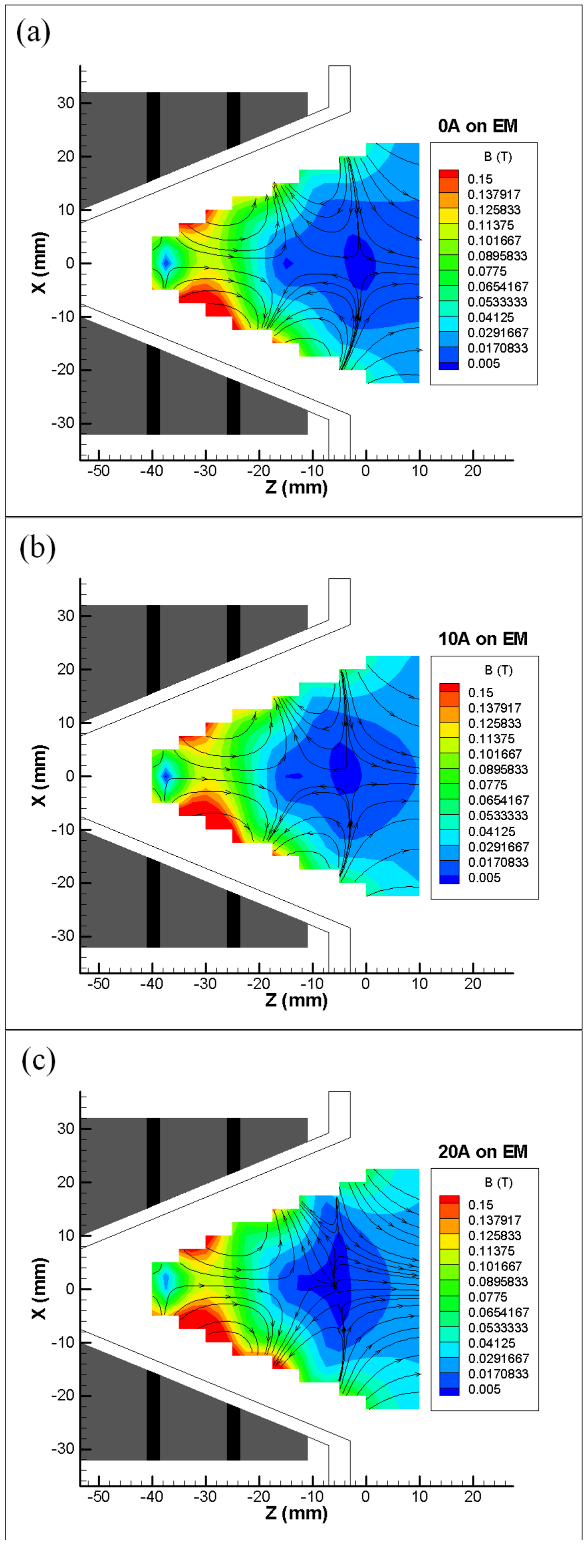

Figure 6. DC Gaussmeter measurements on the DCFT outfitted with electromagnet. Field strength and flux lines are shown in (a) with 0 A (b) 10 A and (c) 20 A supplied to the magnet. The axial distance, Z, is zero at the exit plane defined by the edge of the cap which retains the BN insulating cone.